British Journal of Pharmacology

British Journal of Pharmacology (2018) **175** 3034–3049 3034

RESEARCH PAPER

# LW106, a novel indoleamine 2,3-dioxygenase 1 inhibitor, suppresses tumour progression by limiting stroma-immune crosstalk and cancer stem cell enrichment in tumour micro-environment

**Correspondence** Zhao-Qiu Wu, State Key Laboratory of Natural Medicines, China Pharmaceutical University, Nanjing 211198, China. E-mail: zqwu@cpu.edu.cn

**Received** 16 November 2017; **Revised** 5 April 2018; **Accepted** 19 April 2018

Rong Fu[1,*], Yi-Wei Zhang[1,*], Hong-Mei Li[1,2,*], Wen-Cong Lv[1], Li Zhao[1], Qing-Long Guo[1], Tao Lu[2], Stephen J Weiss[3], Zhi-Yu Li[4] and Zhao-Qiu Wu[1]

[1]*State Key Laboratory of Natural Medicines, Jiangsu Key Laboratory of Carcinogenesis and Intervention, School of Basic Medicine and Clinical Pharmacy, China Pharmaceutical University, Nanjing; Collaborative Innovation Center for Gannan Oil-Tea Camellia Industrial Development, Gannan Medical University, Ganzhou, China,* [2]*Laboratory of Molecular Design and Drug Discovery, School of Science, China Pharmaceutical University, Nanjing, China,* [3]*The Life Sciences Institute, Comprehensive Cancer Center, Division of Molecular Medicine and Genetics, Department of Internal Medicine, University of Michigan, Ann Arbor, USA, and* [4]*Department of Medicinal Chemistry, School of Pharmacy, China Pharmaceutical University, Nanjing, China*

*These authors contributed equally to this work.

## BACKGROUND AND PURPOSE

Indoleamine 2,3-dioxygenase 1 (IDO1) is emerging as an important new therapeutic target for treatment of malignant tumours characterized by dysregulated tryptophan metabolism. However, the antitumour efficacy of existing small-molecule inhibitors of IDO1 is still unsatisfactory and the underlying mechanism remains largely undefined. Hence, we discovered a novel potent small-molecule inhibitor of IDO1, LW106, and studied its antitumour effects and the underlying mechanisms in two tumour models.

## EXPERIMENTAL APPROACH

C57BL6 mice, athymic nude mice or *Ido1*$^{-/-}$ mice were inoculated with IDO1-expressing and -nonexpressing tumour cells and treated with vehicle, epacadostat or increasing doses of LW106. Xenografted tumours, plasma, spleens and other vital organs were harvested and subjected to kynurenine/tryptophan measurement and flow cytometric, histological and immunohistochemical analyses.

## KEY RESULTS

LW106 dose-dependently inhibited the outgrowth of xenografted tumours that were inoculated in C57BL6 mice but not nude mice or *Ido1*$^{-/-}$ mice, showing a stronger antitumour efficacy than epacadostat, an existing IDO1 inhibitor. LW106 substantially elevated intratumoural infiltration of proliferative $T_{eff}$ cells, while reducing recruitment of proliferative $T_{reg}$ cells and non-haematopoietic stromal cells such as endothelial cells and cancer-associated fibroblasts. LW106 treatment resulted in a reduced subpopulation of cancer stem cells (CSCs) in xenografted tumours in which fewer proliferative/invasive tumour cells and more apoptotic tumour cells were observed.

## CONCLUSIONS AND IMPLICATIONS

LW106 inhibits tumour outgrowth by limiting stroma-immune crosstalk and CSC enrichment in the tumour micro-environment. LW106 has potential as a immunotherapeutic agent for use in combination with immune checkpoint inhibitors and (or) chemotherapeutic drugs for cancer treatment.

DOI:10.1111/bph.14351

### Abbreviations

1-MT, 1-methyl-trytophan; CAF, cancer-associated fibroblast; CAM, cancer-associated macrophage; CSC, cancer stem cell; DC, dendritic cell; DMFS, distant-metastasis-free survival; ECM, extracellular matrix; H&E, haematoxylin and eosin; IDO1, indoleamine 2,3-dioxygenase 1; NSCLC, non-small cell lung cancer; OS, overall survival; PBMC, human peripheral blood mononuclear cell; PPS, post-progression survival; TDO, tryptophan 2,3-dioxygenase; TME, tumour micro-environment; α-SMA, α-smooth muscle actin

## Introduction

The intracellular enzyme **indoleamine 2,3-dioxygenase 1 (IDO1)** is a monomeric oxidoreductase that catalyses the first and rate-limiting step in **tryptophan** degradation, leading to subsequent production of bioactive tryptophan metabolites kynurenine (Sono and Hayaishi, 1980; Botting, 1995; Sono *et al.*, 1996). IDO1 has been proposed as a potential contributor to immunosuppression, tolerance and tumour escape from the immune system (Munn *et al.*, 1999; Munn and Mellor, 2004, 2007; Prendergast, 2008). IDO1-mediated depletion of tryptophan and production of kynurenine can lead to an immunosuppressive tumour micro-environment (TME), in which the proliferation of effector T cells is inhibited while suppressive populations of regulatory T cells are activated (Fallarino *et al.*, 2002; Frumento *et al.*, 2002; Munn and Mellor, 2004, 2007). The presence of IDO1 in TME has been shown to correlate with tumour progression, invasion and metastasis and can be used as an independent prognostic marker of survival in various types of cancers (Brandacher *et al.*, 2006; Polak *et al.*, 2007; Ino *et al.*, 2008; Pan *et al.*, 2008). It has been demonstrated that IDO1 is produced mainly by the tumour cells and host-derived immune cells such as dendritic cells (DCs) and macrophages that are recruited to TME by the tumour (Munn *et al.*, 1999; Munn *et al.*, 2002).

The TME is the cellular micro-environment in which the tumour exists, which includes tumour-infiltrating immune cells (e.g. T cells, DCs and macrophages) and non-haematopoietic stromal cells such as cancer-associated fibroblasts (CAFs), endothelial cells (ECs) and pericytes, along with the extracellular matrix (ECM) and inflammatory mediators they secrete (Coussen and Werb, 2002; Johansson *et al.*, 2008; Hanahan and Weinberg, 2011; Hanahan and Coussens, 2012; Turley *et al.*, 2015). There is emerging evidence suggesting that the crosstalk (interaction) between the stromal compartment and immune system within the TME can influence tumour growth, metastasis and chemoresistance (Joyce and Pollard, 2009; Holmgaard *et al.*, 2013). CAFs, the predominant stromal cells, together with ECs and pericytes, enhance the proliferation, extravasation and infiltration of regulatory T cells and reduce the trafficking of proliferative effector T cells to the tumour bed, which can hinder antitumour immune responses and promote tumour progression (Castermans and Griffioen, 2007; Buckanovich *et al.*, 2008; Tan *et al.*, 2011; Feig *et al.*, 2013; Turley *et al.*, 2015). ECM, the non-cellular component in the TME, may also suppress antitumour immune responses and thus support tumour growth by limiting T cell motility (Provenzano *et al.*, 2012; Salmon *et al.*, 2012; Caruana *et al.*, 2015; Turley *et al.*, 2015). However, the stromal immunoregulation in the TME is not unidirectional. A growing body of evidence now exists to suggest that the infiltrating immune cells can actively shape the stromal milieu in the TME, thus highlighting a considerable level of crosstalk (interaction) between stromal and immune cells (Beatty *et al.*, 2011; Lu *et al.*, 2011; Coussens *et al.*, 2013; Turley *et al.*, 2015). Stromal cells and their associated ECM are now known to play an essential role in controlling the expansion of cancer stem cells (CSCs), a population of tumour cells that possess the defining features of clonogenicity and self-renewal, and CSCs are thought to have a critical role in tumour progression, metastasis and chemoresistance (Bhowmich *et al.*, 2004; Turley *et al.*, 2015; Ni *et al.*, 2016).

It is still unclear whether tumour cell-derived IDO1 contributes to tumour progression in patients (Holmgaard *et al.*, 2013). In the present study, we perform a bioinformatic analysis of the relationship between tumour cell-derived *IDO1* expression levels and survival rates in patients using an online tool (http://kmplot.com/analysis/), which is capable of assessing the effect of 54 675 genes on survival using 10 461 cancer samples, including 5143 breast, 1816 ovarian, 2437 lung and 1065 gastric cancer patients with a mean follow-up of 69, 40, 49 and 33 months respectively (Gyorffy *et al.*, 2010, 2012, 2013; Szasz *et al.*, 2016).

IDO1 is emerging as an important new therapeutic target for the treatment of cancer, and three small-molecule inhibitors of IDO1, **1-methyl-tryptophan (1-MT)**, **NLG919** and **epacadostat** are currently in clinical trials for treatment of non-small cell lung cancer (NSCLC), melanoma and other types of cancer (Cady and Sono, 1991; Liu *et al.*, 2010; Jackson *et al.*, 2013). However, the antitumour efficacy of these existing inhibitors is still unsatisfactory and the underlying mechanism remains largely undefined. In the present study, we describe the discovery and characterization of LW106, a structurally novel small-molecule inhibitor of IDO1. We found that LW106 displays a stronger antitumour efficacy as compared with epacadostat, and further revealed that LW106 inhibits tumour growth by limiting the interaction (crosstalk) between the stromal compartment and the immune system and the enrichment of CSCs in the TME. Our data suggest that LW106 can be further developed as a potential immunotherapeutic agent for cancer treatment.

## Methods

### *Mice and human samples*

Eight-week-old male C57BL/6 mice and athymic nude mice were purchased from Qinglongshan Animal Facility in Nanjing, China. Congenic *Ido1*$^{-/-}$ mice on a C57BL/6 strain background were obtained from the Jackson Laboratory. All mice were housed under standard specific-pathogen-free conditions, and all research involving animals strictly complied with protocols approved by the Animal Welfare and Ethics Committee (China Pharmaceutical University). Animal

studies are reported in compliance with the ARRIVE guidelines (Kilkenny *et al.*, 2010; McGrath and Lilley, 2015). Human peripheral blood mononuclear cells (PBMCs) from healthy volunteers were purchased from Nanjing Red Cross Blood Centre.

## Cell culture

HeLa ovarian carcinoma cells, Lewis lung carcinoma cells and B16F10 melanoma cells were purchased from ATCC (Rockefeller, MD, USA) and grown in DMEM supplemented with 10% heat-inactivated FBS and 1% penicillin/streptomycin (Invitrogen, Carlsbad, CA, USA). Cells were tested for mycoplasma contamination each month, and only mycoplasma-negative cells were used. Short tandem repeat DNA fingerprinting analysis was performed in 2016 for authentication of these cells.

## Tumour formation and drug treatment

Tumour xenograft experiments were performed in 8- to 10-week-old mice challenged s.c. with $6 \times 10^5$ Lewis tumour cells or $2 \times 10^5$ B16F10 melanoma cells. Mice were randomly divided into five groups and injected i.p. daily with vehicle alone, LW106 at doses of 20, 40 and 80 $mg \cdot kg^{-1}$ or epacadostat at 80 $mg \cdot kg^{-1}$ at day 6 following initial tumour cell engraftment until termination of the experiment. All compounds were dissolved freshly in sodium citrate buffer prior to each experiment. Tumour volume was measured every 2 days at day 3 post-tumour inoculation using the formula $V = \pi \times \text{length} \times \text{width}^2/6$. Tumours were harvested, weighed and subjected to further analysis.

## FACS analysis

For the T cell assay, xenografted tumours were dissected, minced into small pieces and digested for 45 min at 37°C in 1X HBSS buffer containing 2% FBS, 1 $mg \cdot mL^{-1}$ collagenase I (Sigma-Aldrich, St Louis, Missouri, USA) and 0.5 $mg \cdot mL^{-1}$ dispase (Invitrogen), followed by further digestion in 10-$\mu g \cdot mL^{-1}$ DNase (Invitrogen) for 45 min, and 0.64% ammonium chloride (STEMCELL Technologies, Vancouver, Canada) for 5 min at 37°C; Spleens from tumour-bearing mice were dissected into pieces and dissociated mechanically in D-Hank's buffer (Invitrogen) for 10 min on ice. Cells were filtered through a 70 μm cell strainer (BD Biosciences, Franklin Lakes, NJ, USA), resuspended in 1X HBSS buffer containing 2% FBS and subjected to a gradient centrifugation in Ficoll-Pague (Sigma-Aldrich). Purified lymphocytes were stained using a fixation and permeabilization kit (eBioscience, San Diego, CA, USA) and analysed by FACS analysis to detect the expression of CD45, CD4, CD8, Foxp3 (all from Biolegend, San Diego, CA, USA) and Ki67 (Cell Signaling, Danvers, MA, USA). For the CSC assay, xenografted tumours were dissected into pieces and dissociated enzymatically as described above. Cells were incubated with an antibody cocktail containing CD31, CD45 and Ter119 (STEMCELL Technologies), a secondary biotin-labelled antibody cocktail (STEMCELL Technologies) and magnetic beads (15 min each). The unbound cells ($LIN^-$) were collected and labelled with APC-CD44 or PE-CD144 (both from BD Biosciences) for 30 min at 4°C, followed by DAPI staining for 5 min at 4°C. Cells were washed extensively and subjected to an aldehyde dehydrogenase (ALDH) activity assay using a kit from STEMCELL Technologies, according to the manufacturer's instructions. The labelled cells were subjected to FACS analysis to detect ALDH activity and the expression of CD133 and CD44.

## Lymphocyte and DC co-culture

Lymphocyte and DC co-cultures were performed as described previously with a slight modification (Liu *et al.*, 2010). PBMCs from healthy volunteers were subjected to centrifugal elutriation to obtain monocytes and lymphocytes. The purified monocytes were treated with 10 $ng \cdot mL^{-1}$ human recombinant **IL-4** (R & D Systems, Minneapolis, MN, USA) and 40 $ng \cdot mL^{-1}$ human recombinant **GM-CSF** (R & D Systems) for 5 days, and the floating and loosely attached cells (i.e. $IDO1^-$ immature DCs) were harvested. $IDO1^+$ mature DCs were obtained by treating immature DCs with 50 $ng \cdot mL^{-1}$ human recombinant **IFN-γ** (Peprotech, Rocky Hill, NJ, USA) and 1 $\mu g \cdot mL^{-1}$ **LPS** (Sigma-Aldrich) for an additional 2 days. $IDO1^+$ mature DCs or $IDO1^-$ immature DCs were co-cultured with purified lymphocytes in the presence of vehicle, LW106 or epacadostat for 2- days. Cells were harvested, stained with anti-CD8 antibody (Biolegend) and subjected to FACS analysis.

## Tumoursphere assay

FACS-sorted single cells were plated in ultralow-attachment plates ($2 \times 10^4$ cells per well; Corning, Corning, NY, USA) with serum-free DMEM/F12 medium (Invitrogen), supplemented with B27 (Invitrogen), 20 $ng \cdot mL^{-1}$ **EGF**, 20 $ng \cdot mL^{-1}$ **bFGF** (R & D Systems) and 4 $mg \cdot mL^{-1}$ heparin (Sigma, St Louis, Missouri, USA). Tumourspheres were counted 7 days after plating.

## Tryptophan/kynurenine measurement

Tryptophan/kynurenine measurements were performed as described previously with slight modifications (Liu *et al.*, 2010). To measure IDO1 enzyme activity *in vitro*, HeLa cells were stimulated with 50 $ng \cdot mL^{-1}$ human recombinant IFN-γ for 48 h, and conditioned media were collected, centrifuged to remove cell debris and stored at −20°C for further use. To measure IDO1 enzyme activity *in vivo*, blood and tumours from vehicle- or drug-treated mice were collected and stored at −20°C for further use. Tumours were homogenized in three volumes of normal saline with 0.1% formic acid. Following protein-precipitation extraction with methanol, supernatants of conditioned media, plasma and tumour homogenates were collected and 20 μL of the supernatants were subjected to LC/MS/MS analysis. Aqueous standards were prepared for adjustment of endogenous tryptophan and kynurenine levels.

## Histological and immunohistochemical analyses

For histology, tissues were fixed in 4% paraformaldehyde, embedded in paraffin and sectioned, followed by haematoxylin and eosin (H&E) staining. For immunohistochemical assays, paraffin-embedded sections were deparaffinized, rehydrated and subjected to antigen heat retrieval with citric buffer, pH 6.0 (Vector Laboratories, Burlingame, CA, USA). The sections were treated with 0.5% $H_2O_2$ (Sigma-Aldrich) for 10 min at room temperature and further incubated in

blocking buffer (5% goat serum in PBS) supplemented with primary antibodies against cleaved **caspase 3** (Cell Signaling), Ki67 (Abcam, Cambridge, UK) and p-Histone H3 (Cell Signaling) overnight at 4°C, followed by incubation with biotinylated goat anti-rabbit secondary antibody (Vector Laboratories) at room temperature for 1 h. A standard ABC kit and DAB (Vector Laboratories) were used for the detection of HRP activity. Sections were counterstained with haematoxylin, dehydrated and mounted. In some experiments, sections were incubated in blocking buffer (5% goat serum in PBS) containing primary antibodies against CD31, α-smooth muscle actin (α-SMA) (both from Abcam), K14 (Biolegend) and CD8 (Biolegend) overnight at 4°C, followed by incubation with goat anti-rat Alexa 488, goat anti-rabbit Alexa 488 and goat anti-rabbit Alexa 594 secondary antibodies (all from Invitrogen) for 1 h at room temperature. Sections were stained with DAPI for 5–10 min at room temperature and mounted for confocal microscopy.

### *Immunoblotting assay*

Cells were harvested and lysed in RIPA buffer (Thermo Scientific) containing proteinase inhibitor cocktail (Thermo Scientific) on ice for 20 min, followed by centrifugation for 20 min at 4°C, 14 000 *g*. The supernatants were collected and subjected to immunoblotting assay using anti-IDO1 antibody (Merck).

### *Cell survival assay*

Tumour cells were seeded in 12-well culture plates and treated with vehicle or the indicated compounds at different concentrations for 2 days. Cells were harvested, resuspended in trypan blue staining buffer (containing 0.04% trypan blue, Thermo Fisher) and cultured for 3 min at room temperature. Live cells (i.e. cells that excluded trypan blue) were instantly counted under light microscope, and survival rates of cells were calculated.

### *Kaplan–Meier survival analysis*

Overall survival (OS), post-progression survival (PPS) and distant-metastasis-free survival (DMFS) rates were assessed in lung cancer patients (with indicated subtypes; Gyorffy *et al*., 2010), ovarian cancer patients (Gyorffy *et al*., 2012), breast cancer patients (Gyorffy *et al*., 2013) and gastric cancer patients (Szasz *et al*., 2016). The patients were divided into 'high' and 'low' groups by median *IDO1* expression. All other parameters were left as default settings.

### *Statistical analysis*

All results wherever necessary were subjected to statistical analysis. Data are presented as mean ± SEM. Statistical analysis was performed as described in each corresponding figure legend. Sample sizes are shown in each corresponding figure legend. $P < 0.05$ was considered significant. The data and statistical analysis comply with the recommendations on experimental design and analysis in pharmacology (Curtis *et al*., 2015).

### *Chemical compounds*

LW106 (MW: 245; Figure S1) was synthesized at the Department of Medicinal Chemistry, School of Pharmacy, China Pharmaceutical University, and the purity was no less than 99%. Using the binding model of the lead compound 62 with IDO1 (PDB code: 2D0T) by molecular docking, we probed the active site and discovered more potent IDO inhibitors based on 62. It was observed oximido of 62 could interact with haem 7-propionic acid to form a conserved hydrogen contributing greatly to the strong protein occupancy. The oxadiazole of 62 is directed towards the backup hydrophobic pocket ($Arg^{231}$, $Phe^{226}$) and forms a strong cation−π interaction with $Arg^{231}$ of the protein. While the benzyl group of 62 is oriented towards the small hydrophobic pocket, away from the haem iron and thus lacking any specific interaction with the protein. We hypothesized that replacement of the imine (62) with heterocycles (LW106) to occupy the deep space and stabilize the conformation of the compound might have a favourable contribution to the affinity improvement. Epacadostat was purchased from MedChem Express. Stock solutions and prepared in DMSO for use in cell-based assays.

### *Nomenclature of targets and ligands*

Key protein targets and ligands in this article are hyperlinked to corresponding entries in http://www.guidetopharmacology.org, the common portal for data from the IUPHAR/BPS Guide to PHARMACOLOGY (Harding *et al*., 2018), and are permanently archived in the Concise Guide to PHARMACOLOGY 2017/18 (Alexander *et al*., 2017).

## Results

### *Tumour cell-derived IDO1 expression level does not correlate with cancer patient survival*

To date, it is still controversial whether tumour cell-derived *IDO1* expression level correlates with cancer patient survival (Holmgaard *et al*., 2013). Using a Kaplan–Meier survival analysis (http://kmplot.com/analysis/), we failed to observe a statistically significant relationship between OS, PPS and DMFS rates and tumour cell-derived *IDO1* expression level in patients with various types of cancers such as lung, ovarian, breast or gastric cancer (Figure 1A–H; Figure S2A–D). These data suggest that targeting IDO1 as a therapeutic strategy might be applicable to IDO1-expressing host-derived cells but not tumour cells.

### *LW106 inhibited IDO1 enzyme activity but did not affect tumour cell proliferation in vitro*

To determine the *in vitro* inhibitory effect of LW106 on IDO1 enzyme activity, HeLa ovarian carcinoma cells were stimulated with IFN-γ and applied to an enzyme activity assay. It has been reported that expression level of IDO1 but not IDO2 or **tryptophan 2,3-dioxygenase (TDO2)** was dramatically increased in the stimulated cells (Liu *et al*., 2010). We observed that LW106 inhibited IDO1 enzyme activity with an $IC_{50}$ value of 1.57 μM while did not affect IDO1 protein expression level in the stimulated cells (Figure S3A, B). Moreover, LW106 at doses ranging from 12.5 to 200 μM did not affect proliferation of three types of tumour cells with different expression levels of IDO1 (Figure S3C–E). It has been reported that $IDO1^{+}$ DCs can inhibit T-cell proliferation/survival, which is believed to be responsible

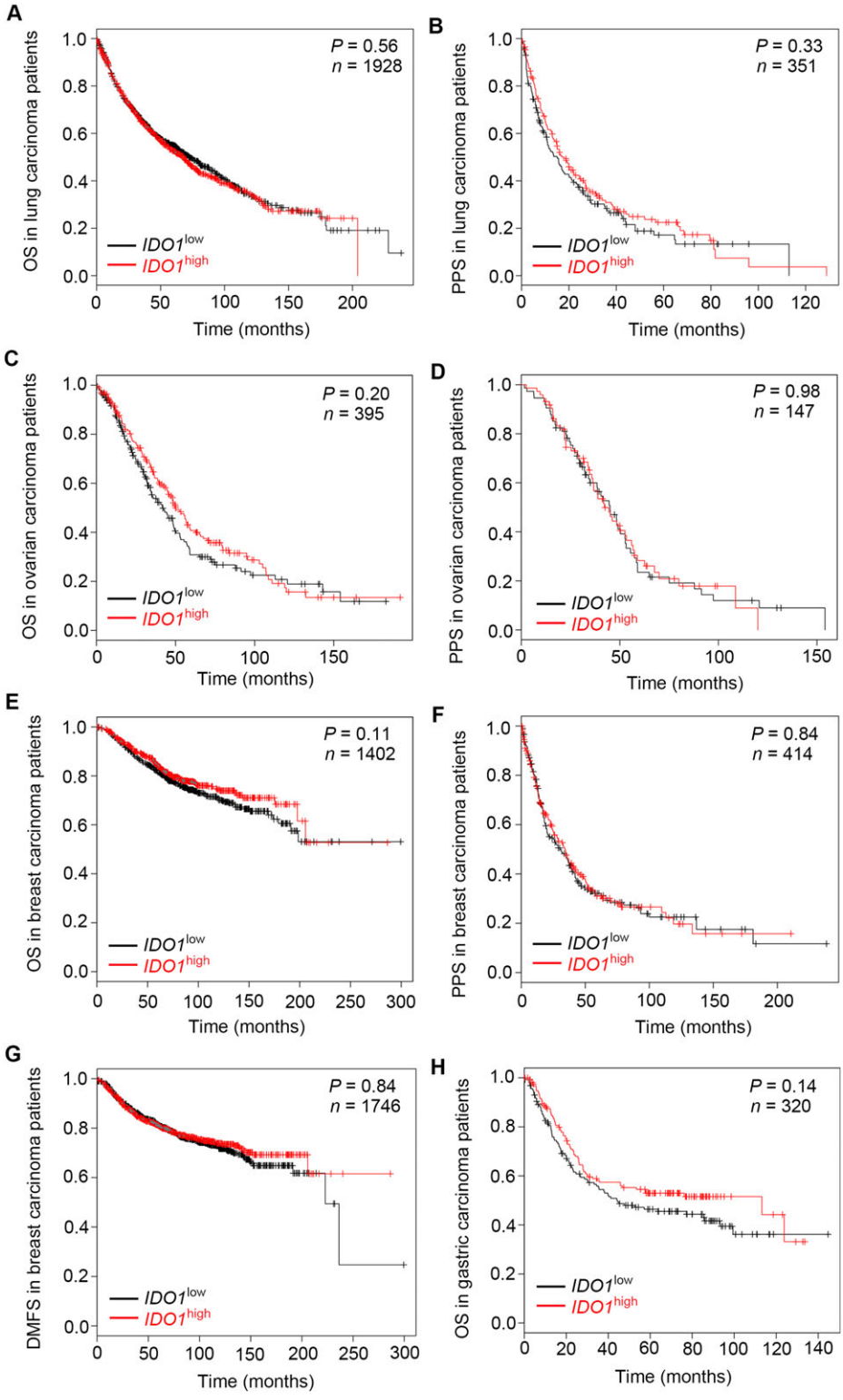


## Figure 1

Tumour cell-derived *IDO1* expression level does not correlate with cancer patient survival. Kaplan–Meier survival analysis of the relationship between survival rates and tumour cell-derived *IDO1* expression level in patients with various types of cancers. (A, B) Relationship between OS (A) and PPS (B) rates and *IDO1* expression level in lung cancer patients. (C, D) Relationship between OS (C) and PPS (D) rates and *IDO1* expression level in ovarian cancer patients. (E–G) Relationship between OS (E), PPS (F) and DMFS (G) rates and *IDO1* expression level in breast cancer patients. (H) Relationship between OS rate and *IDO1* expression level in gastric cancer patients. Differences between two survival curves are measured by Log-Rank Test. *n* represents the number of patients.

for IDO1-mediated tumour escape (Mellor *et al.*, 2003). To examine whether LW106 could reverse IDO1-mediated T-cell suppression, $IDO1^+$ mature DCs or $IDO1^-$ immature DCs were co-cultured with purified lymphocytes in the presence of vehicle, LW106 or epacadostat. Co-cultured cells were harvested, stained with anti-CD8 antibody and subjected to FACS analysis. We found that IDO1 induction strongly suppressed $CD8^+$ T-cell proliferation/survival in the co-culture system, and the suppression could be effectively reversed by LW106 and epacadostat (Figure S4A, B).

## *LW106 dose-dependently inhibited the outgrowth of IDO1-expressing tumour cells inoculated in immunocompetent C57BL6 mice but not athymic nude mice or Ido1$^{-/-}$ mice*

To further determine the inhibitory effect of LW106 on outgrowth of tumour cells *in vivo*, immunocompetent C57BL6 mice were challenged with IDO1-expressing Lewis lung carcinoma cells and treated with various doses of LW106 or epacadostat, an existing potent small molecule inhibitor of IDO1 that is currently in clinical trial for cancer treatment. We observed that LW106 dose-dependently inhibited tumour growth, reducing tumour weights by 30, 54 and 68% at 20, 40 and 80 mg·kg$^{-1}$ respectively (Figure 2A). Importantly, we failed to observe pathological changes in vital organs (e.g. heart, liver, lung and kidney) of mice that received LW106 treatment at 80 mg·kg$^{-1}$ (Figure S3A). Meanwhile, epacadostat treatment at 80 mg·kg$^{-1}$ reduced tumour weight by 51%, displaying a weaker antitumour efficacy as compared with LW106 (Figure 2A). Similarly, a significant reduction in tumour volumes was observed in LW106-treated mice relative to vehicle-treated mice (Figure 2B). A marked reduction in kynurenine/tryptophan ratio was also detected in plasmas and xenografts of LW106-treated mice (Figure 2C). However, it should be noted that tryptophan depletion and **GCN2** kinase activation may also play important roles in IDO1-mediated tumour immune escape (Munn *et al.*, 2005; Eleftheriadis *et al.*, 2014). Of note, both LW106- and epacadostat-treated mice displayed markedly increased survival compared with vehicle-treated mice (Figure 2D). It has been documented that IDO1 enzyme inhibitors require intact T-cell function to suppress tumour growth in mice (Liu *et al.*, 2010). To evaluate the importance of T-cell-dependent immunity to the antitumour effect of LW106, athymic nude mice that are deficient in mature T cells were challenged with Lewis tumour cells and tumour outgrowth were monitored. In the context of these mice, LW106 treatment at 80 mg·kg$^{-1}$ had no distinguished effect on tumour outgrowth, suggesting that LW106 exerts its antitumour effect in a T-cell-dependent manner (Figure 2E). We further applied *Ido1*$^{-/-}$ (*Ido1* knockout) mouse model to determine whether IDO1 blockade in the inoculated tumour cells or the host-derived cells is directly relevant to the mechanism of antitumour effect of LW106. Interestingly, we found that LW106 treatment at 80 mg·kg$^{-1}$ failed to suppress tumour outgrowth in *Ido1*$^{-/-}$ mice that were inoculated with IDO1-expressing Lewis tumours, suggesting that LW106 inhibited tumour outgrowth via blocking activity of IDO1 expressed by the host-derived cells but not the inoculated tumour cells (Figure 2F).

## *LW106 dose-dependently inhibited outgrowth of IDO1-nonexpressing tumour cells inoculated in C57BL6 mice but not athymic nude mice or Ido1$^{-/-}$ mice*

We extended our studies to further evaluate LW106 treatment in another widely used B16F10 melanoma tumour model (IDO1 is undetectable in B16F10 cells). Again, we observed that tumour weights were reduced by 29, 52 and 65% in mice treated with LW106 at 20, 40 and 80 mg·kg$^{-1}$ respectively (Figure 3A). We did not observe pathological changes in vital organs (e.g. heart, liver, lung and kidney) of mice that received LW106 treatment at 80 mg·kg$^{-1}$ (Figure S5A, B). Epacadostat displayed a weaker antitumour efficacy than LW106, with a 50% reduction in tumour weight when administrated at 80 mg·kg$^{-1}$ (Figure 3A). Additionally, a substantial decrease in tumour volumes was observed in LW106-treated mice relative to vehicle-treated mice (Figure 3B). LW106 treatment at 80 mg·kg$^{-1}$ did not suppress outgrowth of B16F10 tumours that were inoculated in athymic nude mice or *Ido1*$^{-/-}$ mice (Figure 3C, D), further support the notion that T-cell immunity and IDO1 targeting in the host-derived cells are essential for antitumour efficacy of LW106.

## *LW106 treatment enhanced the infiltration and accumulation of T cells in xenografted tumours*

Given that T-cell-dependent immunity is essential for tumour-suppressive activity of LW106, we sought to study the effector T cell and regulatory T cell compartments within the Lewis and B16F10 tumours following LW106 treatment. For this purpose, tumours were harvested 18 days after implantation, and tumour-infiltrating lymphocytes were isolated and subjected to FACS analysis. We observed a significantly increased number of tumour-infiltrating CD8 effector T cells ($CD8^+CD45^+$) in mice treated with LW106 as compared with vehicle-treated mice (Figure 4A; Figure S6A). LW106 treatment also increased infiltration of proliferative CD8 effector T cells within the xenografted tumours, as measured by expression of Ki67, a widely used cell proliferating marker (Figure 4B). By contrast, infiltration of regulatory T cells ($CD4^+Foxp3^+CD45^+$) was robustly reduced in LW106-treated mice relative to vehicle-treated mice (Figure 4C). A dramatic decrease in the percentage of proliferative regulatory T cells was observed within xenografted tumours of LW106-treated mice (Figure 4D; Figure S6B). Intratumoural ratios of CD4 effector T cells ($CD4^+Foxp3^-CD45^+$) to regulatory T cells were markedly elevated in LW106-treated mice as compared with vehicle-treated mice (Figure 4E; Figure S6C). Additionally, immunofluorescence analysis further revealed a robustly increased infiltration of proliferative CD8 effector T cells ($Ki67^+CD8^+$) within xenografted tumours of LW106-treated mice (Figure 4F; Figure S6D).

## *LW106 treatment enhanced accumulation of splenic T cells in Lewis tumour-bearing mice*

Because spleen serves as an important reservoir for lymphocytes that can be recruited to the tumour sites and directly involve in antitumour immunity, we therefore sought to study the effector T cell and regulatory T cell compartments in the spleens of tumour-bearing mice. We observed markedly

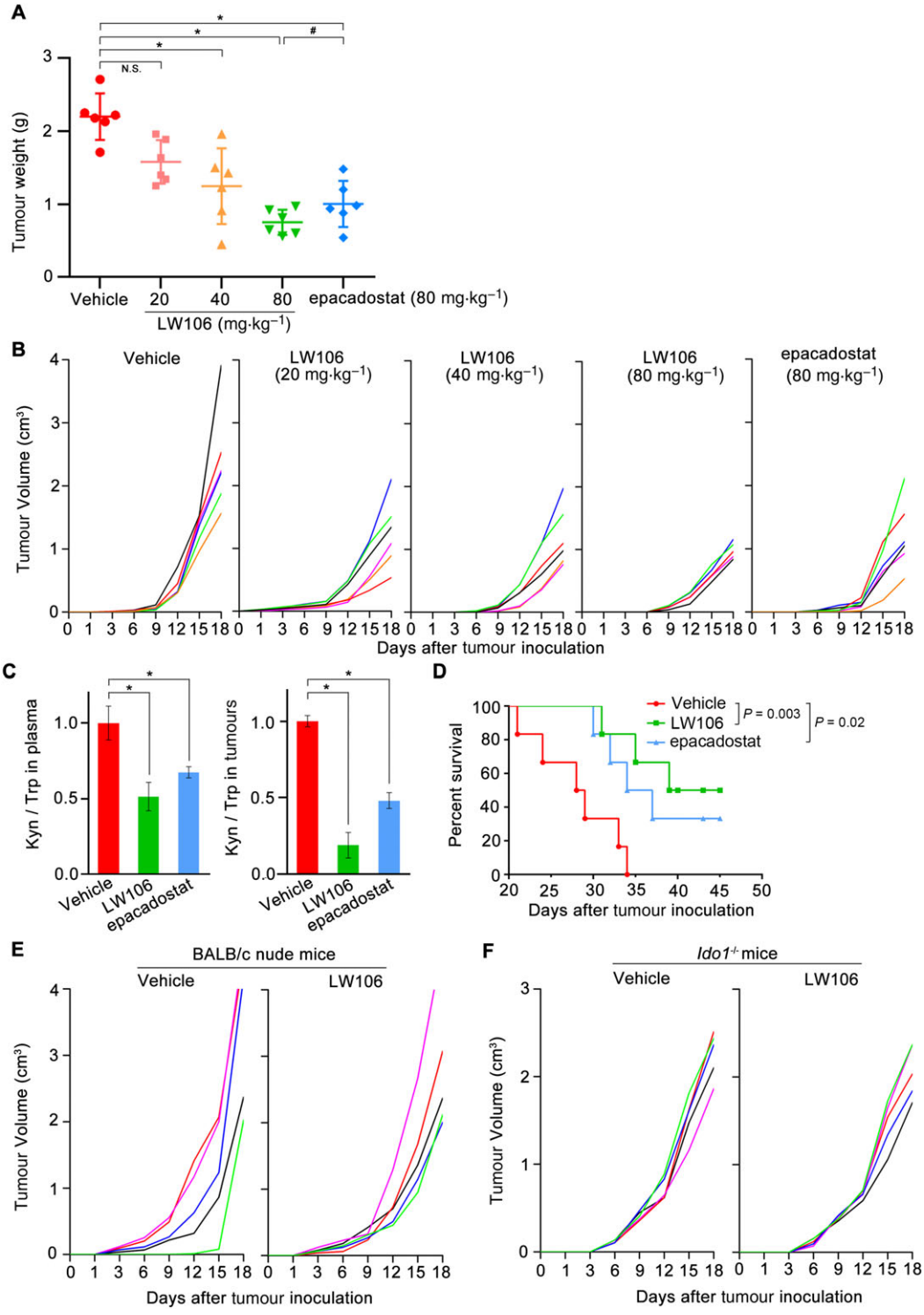


## Figure 2

Lewis tumour outgrowth suppression by LW106 depends on T cells and IDO1 targeting. Mice were administered the indicated compounds, i.p. daily, at day 6 following s.c. challenge with $6 \times 10^5$ Lewis tumour cells. (A) Tumour weights in immunocompetent mice ($n = 6$ mice, each). (B) Individual tumour growth in immunocompetent mice ($n = 6$ mice, each). (C) Ratio of tryptophan to kynurenine concentration in plasma and xenografted tumours from immunocompetent mice ($n = 6$ mice, each). (D) Kaplan–Meier survival curves for tumour-bearing mice that were treated with vehicle, LW106 and epacadostat ($n = 6$ mice, each). (E, F) Individual tumour growth in BALB/c nude mice (E) and *Ido1*$^{-/-}$ mice (F) ($n = 5$ mice, each). Statistical significance was evaluated by two-way ANOVA test (A, B, C, E and F; $^*P < 0.05$; $^{\#}P < 0.05$) and Log-Rank test (D).

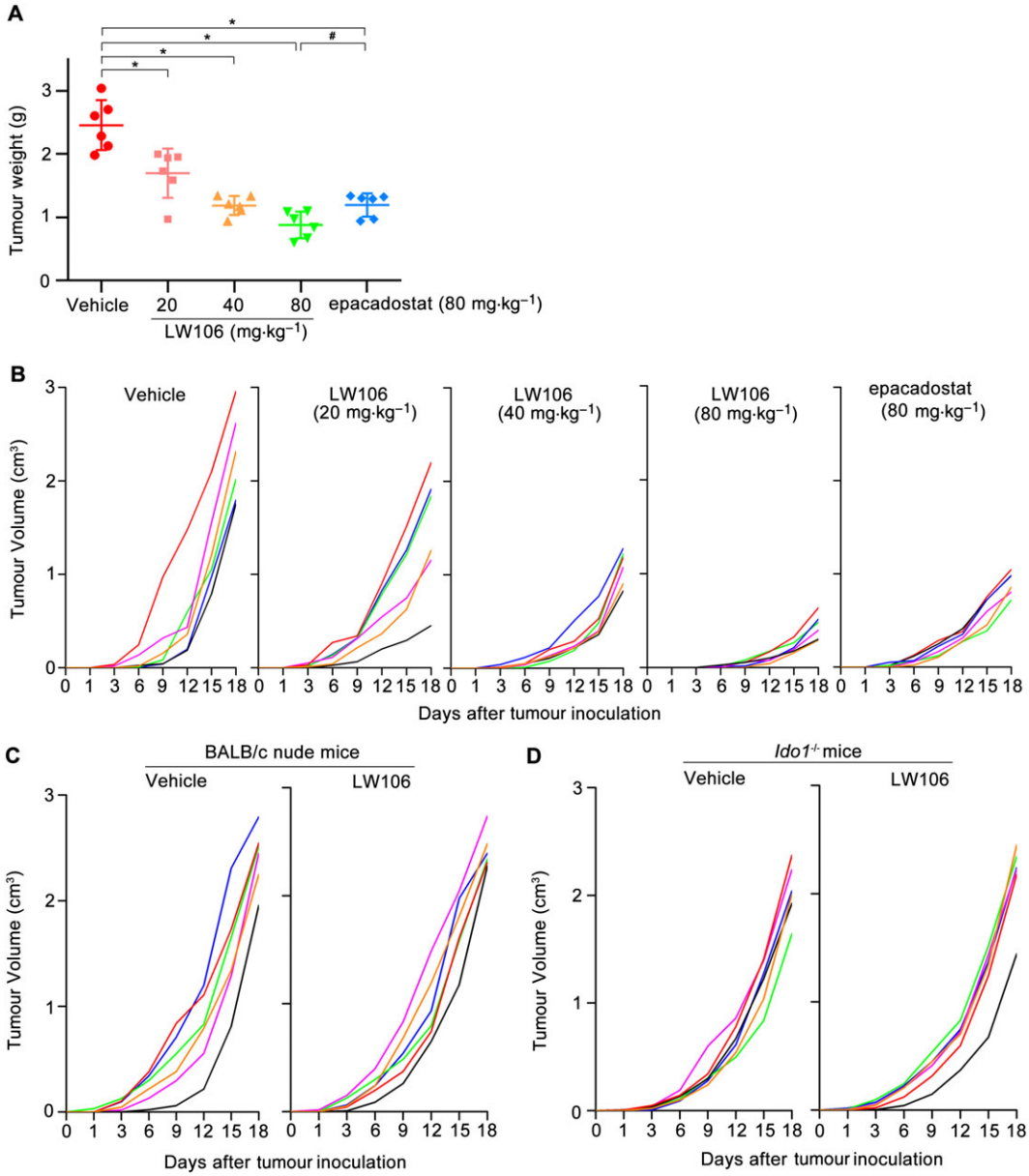


## Figure 3

B16F10 melanoma outgrowth suppression by LW106 is dependent on T cells and IDO1. Mice were administered the indicated compounds, i.p. daily, at day 6 following s.c. challenge with $2 \times 10^5$ B16F10 melanoma cells. (A) Tumour weights in immunocompetent mice ($n = 6$ mice, each). (B) Individual tumour growth in immunocompetent mice ($n = 6$ mice, each). (C, D) Individual tumour growth in BALB/c nude mice (C) and *Ido1*$^{-/-}$ mice (D) ($n = 5$ mice, each). Statistical significance was evaluated by two-way ANOVA test ($^*P < 0.05$; $^{\#}P < 0.05$).

enlarged spleens in mice that received LW106 treatment as compared with epacadostat- or vehicle-treated mice (Figure 5A, B). Importantly, H&E staining of spleens from LW106-treated mice revealed no distinguished pathological changes (Figure 5C). Flow cytometry analysis of splenocytes revealed a higher percentage of CD8 effector T cells in the spleens of LW106-treated mice as compared to vehicle-treated mice (Figure 5D). Furthermore, LW106 treatment significantly increased the percentage of proliferative CD8 and CD4 effector T cells in tandem with a marked reduction in the percentage of proliferative regulatory T cells in the spleens (Figure 5E–G). Taken together, these results suggest that LW106 treatment increased the number of splenic effector T cells that can be recruited to the tumour sites and function there.

### *LW106 treatment resulted in impaired proliferation and survival of tumour cells in tandem with reduced recruitment of non-haemopoietic stromal cells and deposition of ECM in the TME*

The data above had shown that tumour outgrowth was significantly inhibited in LW106-treated mice. We next

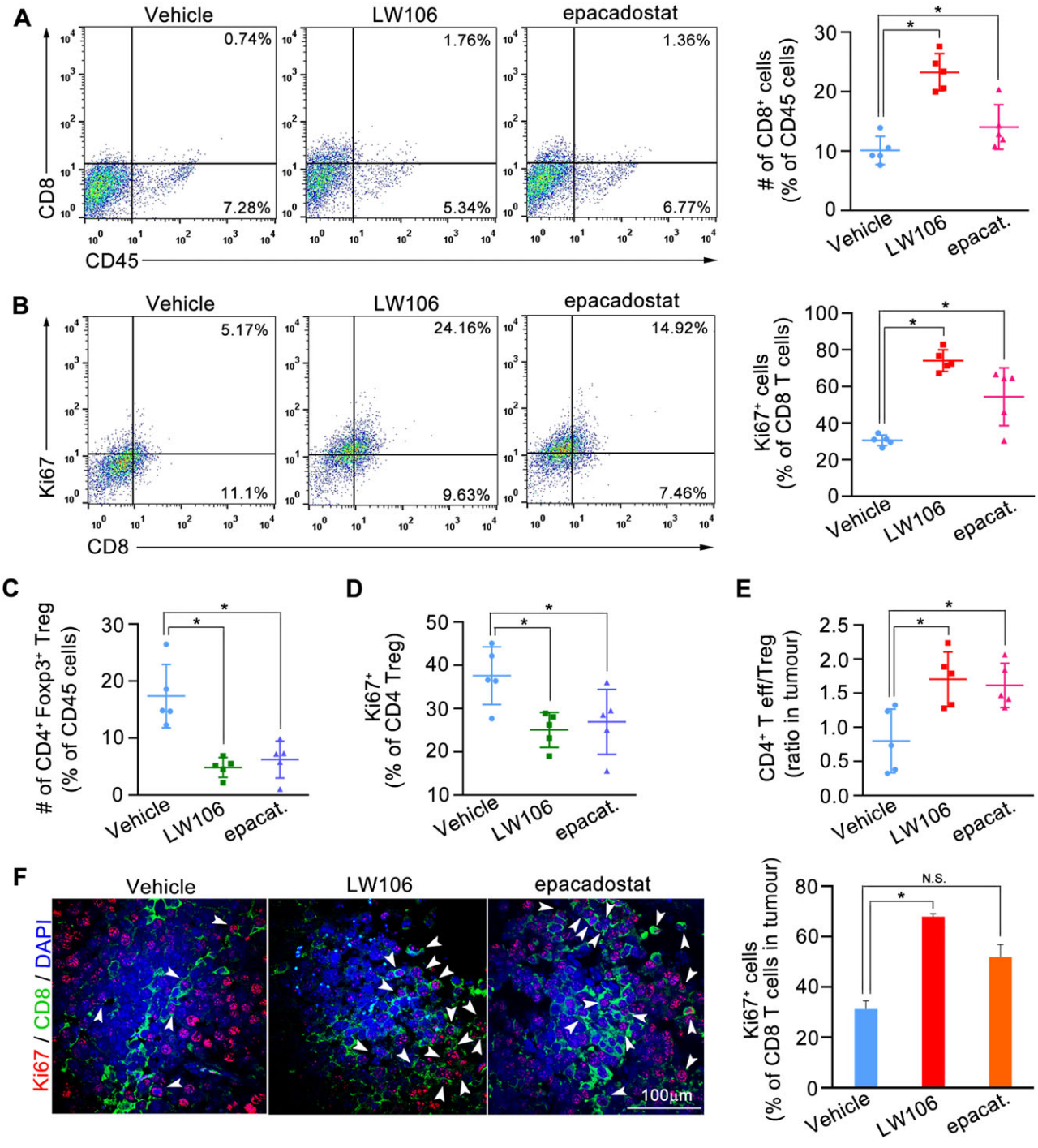


## Figure 4

LW106 treatment enhances the infiltration and accumulation of T cells in xenografted tumours. Lewis tumours from vehicle-, LW106- and epacadostat-treated mice were harvested 18 days after tumour inoculation and subjected to FACS and immunofluorescent analyses. (A) Representative dot plots and percentage of $CD8^+$ effector T cells of total $CD45^+$ cells for vehicle-, LW106- and epacadostat-treated mice ($n$ = 5 mice, each). (B) Representative dot plots and percentage of $CD8^+$ effector T cells expressing Ki67 for indicated mice, as shown in (A). (C) Percentage of $CD4^+Foxp3^+$ regulatory T cells of total $CD45^+$ cells for indicated mice, as shown in (A). (D) Percentage of $CD4^+Foxp3^+$ regulatory T cells expressing Ki67 for indicated mice, as shown in (A). (E) Ratio of $CD4^+Foxp3^-$ effector T cells to $CD4^+Foxp3^+$ regulatory T cells in tumours of indicated mice, as shown in (A). (F) Representative immunofluorescent images (left panels; images are representative of images from five mice) and percentage of $CD8^+$ T cells expressing Ki67 for tumours of indicated mice (right panel; 1000–2000 cells were counted in 10 random fields from each slide). Arrow head denotes $Ki67^+CD8^+$ cells. Statistical significance was evaluated by two-way ANOVA test (*$P < 0.05$; N.S., not significant).

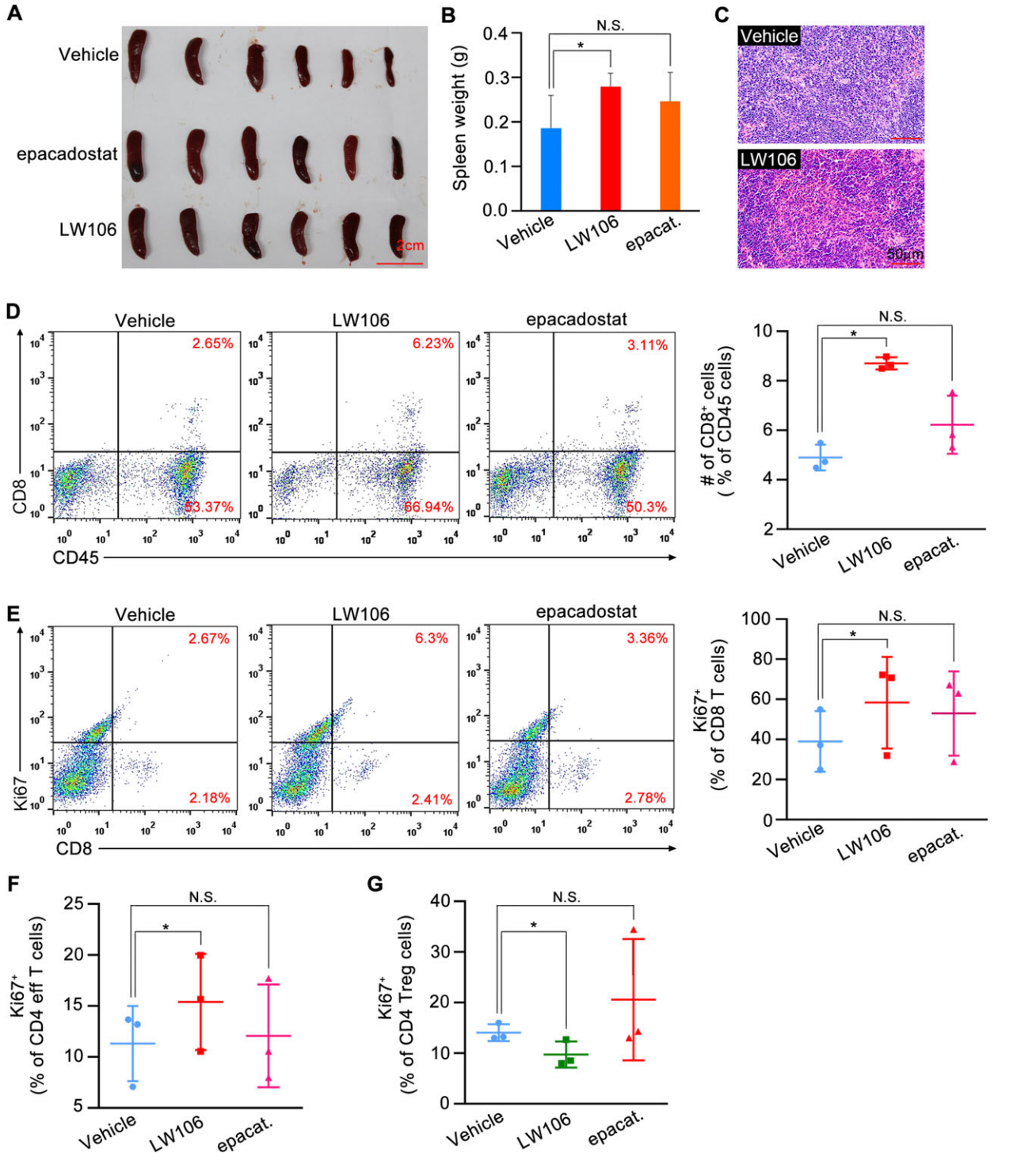


## Figure 5

LW106 treatment enhances the accumulation of splenic T cells in Lewis tumour-bearing mice. Spleens from Lewis tumour-bearing mice that were treated with vehicle, LW106 and epacadostat were harvested and subjected to FACS and histological analyses. (A) Gross examination of spleens from tumour-bearing mice that were treated with the indicated compounds ($n$ = 6 mice, each). (B) Spleen weights in tumour-bearing mice as shown in (A). (C) H&E staining of spleens as shown in (A). (D) Representative dot plots and percentage of $CD8^+$ effector T cells of total $CD45^+$ cells for spleens of tumour-bearing mice that were treated with the indicated compounds ($n$ = 6 mice in three pools, each). (E) Representative dot plots and percentage of $CD8^+$ effector T cells expressing Ki67 for spleens of tumour-bearing mice as shown in (D). (F, G) Percentages of $CD4^+Foxp3^-$ effector T cells (F) and $CD4^+Foxp3^+$ regulatory T cells (G) expressing Ki67 for spleens of tumour-bearing mice as shown in (D). Statistical significance was evaluated by two-way ANOVA test (*$P < 0.05$; N.S., not significant).

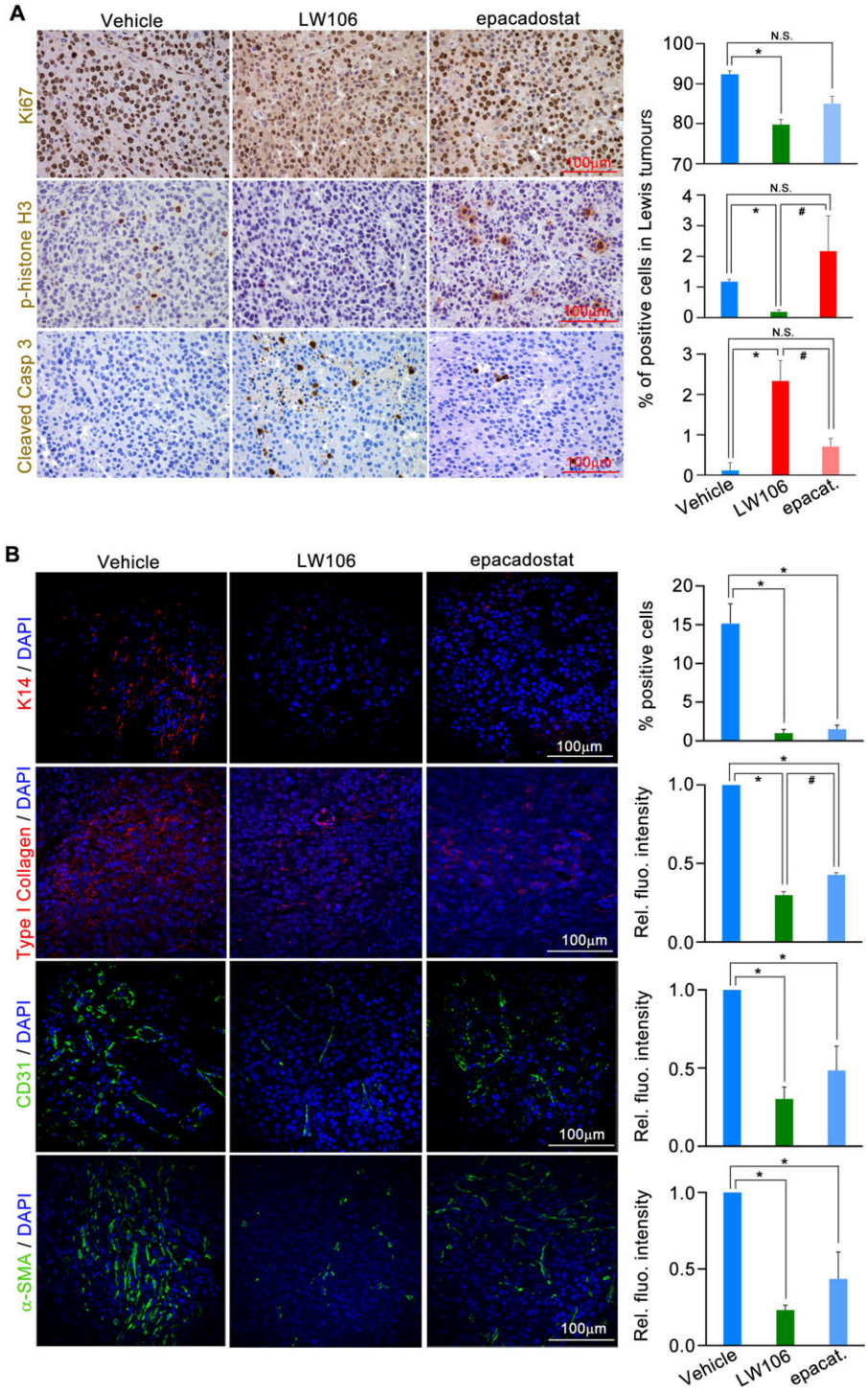


## Figure 6

LW106 treatment results in impaired proliferation and survival of Lewis tumour cells in tandem with reduced recruitment of tumour-associated stromal cells and accumulation of extracellular matrix. Lewis xenografted tumours from vehicle-, LW106- and epacadostat-treated mice were harvested 18 days after tumour challenge and analysed by immunohistochemistry. (A) Representative immunohistochemical images (left panels; images are representative of images from six mice) and percentages of Ki67-, phospho-histone H3- and cleaved caspase 3-positive cells for tumours of indicated mice (right panels; 1000–2000 cells were counted in 10 random fields of each slide). (B) Representative immunofluorescent images (left panels; images are representative of images from six mice), percentage of Ki67-positive cells (1st row at right panels; 1000–2000 cells were counted in 10 random fields of each slide) and relative fluorescent intensities of type I collagen, CD31 and α-SMA (rest rows at right panels; relative fluorescent intensities were calculated in 10 random fields of each slide) for tumours of indicated mice ($n = 6$ mice, each). Statistical significance was evaluated by two-way ANOVA test (*$P < 0.05$; $^{\#}P < 0.05$; N.S., not significant).

sought to determine whether LW106 treatment could affect the proliferation and survival of tumour cells within Lewis and B16F10 tumours. For this purpose, we performed immunohistochemical staining of Ki67 (a proliferative cell marker), phospho-Histone H3 (a mitotic cell marker) and cleaved caspase 3 (an apoptotic cell marker) in the xenografted tumours. We found that the percentages of proliferative and mitotic cells were markedly decreased in tumours of LW106-treated mice relative to vehicle-treated mice (Figure 6A; Figure S7A). By contrast, the percentage of apoptotic cells was significantly increased in tumours of LW106-treated mice (Figure 6A; Figure S7A). A reduced number of cytokeratin-14 (K14)-positive tumour cells (i.e. invasive tumour cells) was also observed in tumours of LW106-treated mice (Figure 6B). These data suggest that LW106 treatment decreases the proliferation, survival and invasiveness of tumour cells, thus suppressing tumour outgrowth.

The relationship between the stroma and tumour-infiltrating lymphocytes remains largely uncharacterized (Turley *et al*., 2015). Emerging evidences have suggested that the stromal compartments (e.g. CAFs, ECs as well as ECM) can shape antitumour immunity and responsiveness to immunotherapy (Turley *et al*., 2015). We therefore sought to determine whether LW106 treatment could affect the recruitment of non-haematopoietic stromal cells and the deposition of stroma-derived ECM in the TME, which may contribute to its antitumour effect. Immunohistochemical assay showed that type I collagen expression level was significantly decreased in tumours of LW106-treated mice, indicating a reduced ECM deposition in the tumours following LW106 treatment (Figure 6B; Figure S7B). We further observed that the percentages of CD31-positive cells (i.e. ECs) and α-SMA-positive cells (i.e. CAFs) were substantially reduced in tumours of LW106-treated mice as compared with vehicle-treated mice (Figure 6B; Figure S7B). These data illustrated that targeting IDO1 in host-derived cells by LW106 inhibited recruitment of non-haematopoietic stromal cells and deposition of ECM, which could generate a tumour-suppressive microenvironment within the tumours and thus suppress tumour outgrowth.

### *LW106 treatment inhibited enrichment of CSCs in xenografted tumours*

CSCs, a population tumour cells that possess the defining features of clonogenicity and self-renewal, are proposed to have a critical role in tumour progression, metastasis and drug resistance (Codony-Servat *et al*., 2016; Hardavella *et al*., 2016; Ni *et al*., 2016). CSCs in human lung tumours were identified using a list of markers such as CD133, CD44 and ALDH1 (Codony-Servat *et al*., 2016; Hardavella *et al*., 2016). To test whether these markers could also be used for identification of CSCs in Lewis xenografted tumours, we sorted tumour cells using FACS with these markers and performed *in vitro* tumoursphere assays. Although we could not detect CD133 expression in the xenografted tumours (data not shown), we indeed observed that $ALDH^+$ or $CD44^+ALDH^+$ cells possessed the potentials to form tumoursphere (Figure 7A). These results suggest that both CD44 and ALDH1 can be used as markers for identification of CSCs in Lewis xenografted tumours. We further found that xenografted tumours of LW106-treated mice displayed markedly reduced numbers of $CD44^+$, $ALDH^+$ or $CD44^+ALDH^+$ cells as compared with vehicle-treated mice (Figure 7B), which may be attributed to the regression of tumours observed in LW106-treated mice (Figure 2A).

## Discussion

Inhibition of IDO1 is a very promising area of cancer immunotherapy. Three small-molecule inhibitors of IDO1, 1-MT, NLG919 and epacadostat, are currently in clinical trials for treatment of various types of cancer including NSCLC, ovarian cancer and melanoma (Cady and Sono, 1991; Liu *et al*., 2010; Jackson *et al*., 2013). These compounds possess potential immunomodulating and antineoplastic activities by inhibiting IDO1 enzyme activity in the tumour cells and host-derived immune cells such as DCs and macrophages (Cady and Sono, 1991; Liu *et al*., 2010; Jackson *et al*., 2013). In the present study, we have discovered LW106 as a structurally novel, selective and potent small-molecule inhibitor of IDO1. In comparison with epacadostat, LW106 showed a weaker *in vitro* inhibition on IDO1 enzyme activity when assayed in IFN-γ-stimulated HeLa cells but indeed displayed a stronger antitumour efficacy in mice bearing xenografted tumours. It is unlikely that the antitumour activity of LW106 is due to the 'off-target' effect as the compound does not suppress tumour outgrowth in *Ido1*$^{-/-}$ mice. A possible explanation for the distinguished inhibition performed by LW106 *in vitro* versus *in vivo* is that LW106 might be metabolized into potential metabolite(s) *in vivo* that can inhibit IDO1 enzyme activity more efficiently than LW106 itself, and further work is required to identify and synthesize the potential metabolite(s) and evaluate their antitumour efficacy. Nevertheless, LW106 can be considered as a potent and selective inhibitor of IDO1 since treatment with the compound causes a strong tumour regression in IDO1-intact mice but fails to inhibit tumour outgrowth in IDO1-deficient mice.

Inhibition of IDO1 enzyme activity in tumour cells appears not to affect cell growth *in vitro* as tumour cells grow normally when treated with LW106 at a concentration of over 100-fold higher than $EC_{50}$. The inhibitory effect of LW106 on tumour outgrowth *in vivo* is related to IDO1 expression by host-derived immune cells but not tumour cells since LW106 administrated *in vivo* display a comparable inhibitory effect on proliferation of IDO1-expressing xenografts versus IDO1-nonexpressing xenografts. In addition, Kaplan–Meier survival analysis reveals that the mRNA levels of IDO1 expressed by tumour cells do not correlate with the survivals in patients with various types of cancers such as lung, ovarian, breast or gastric cancer. Hence, it is reasonable to propose that IDO1 expression by host-derived cells rather than tumour cells can be used as a predictive marker for response to therapy with LW106 as well as other selective inhibitors of IDO1 such as NLG919 (Jackson *et al*., 2013) and epacadostat (Liu *et al*., 2010) and that such immunotherapy can also be beneficial for patients with undetectable IDO1 expression in tumour cells.

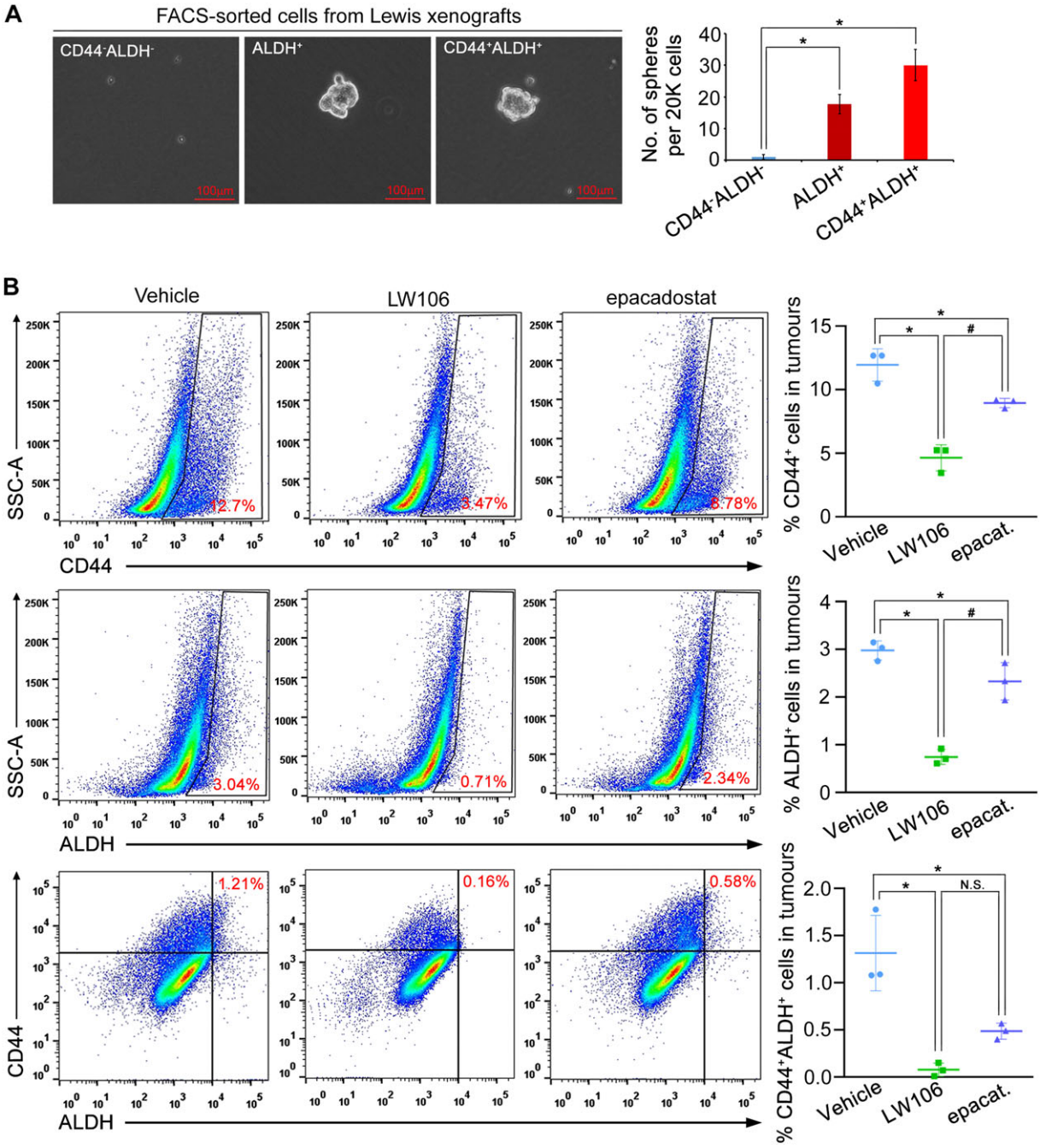


## Figure 7

LW106 treatment inhibits cancer stem cell enrichment in Lewis tumours. Tumours from vehicle-, LW106- and epacadostat-treated mice were harvested 18 days after tumour challenge and subjected to FACS and tumoursphere assays. (A) Representative tumoursphere images (left panels; images are representative of images from six xenografted tumours in three pools) and number of tumourspheres formed by FACS-sorted $CD44^{-}ALDH^{-}$, $ALDH^{+}$ and $CD44^{+}ALDH^{+}$ tumour cells of Lewis xenografts (right panels; $n = 3$ independent experiments). (B) Representative dot plots (left panels; plots are representative of plots from six mice in three pools) and percentages of $CD44^{+}$, $ALDH^{+}$ and $CD44^{+}ALDH^{+}$ cancer stem cells for tumours of indicated mice (right panels; $n = 6$ mice in three pools). Statistical significance was evaluated by two-way ANOVA test ($^{*}P < 0.05$; $^{\#}P < 0.05$).

Emerging evidence suggests that the stromal compartment in the TME may hinder antitumour immune response via actively interacting with the surrounding immune cells (Joyce and Pollard, 2009; Turley *et al.*, 2015). For instance, non-haematopoietic stromal cells such as CAFs and ECs express numerous surface and secreted molecules to directly suppress $CD4^{+}$ and $CD8^{+}$ effector T cells and activate suppressive myeloid cells and $CD4^{+}$ regulatory T cells (Castermans and Griffioen, 2007; Buckanovich *et al.*, 2008; Joyce and Pollard, 2009; Tan *et al.*, 2011; Feig *et al.*, 2013). The stroma-

derived ECM in the TME may also suppress antitumour immune response by limiting T cell motility and localization (Joyce and Pollard, 2009; Provenzano *et al.*, 2012; Salmon *et al.*, 2012; Caruana *et al.*, 2015). Of note, immune cells including regulatory T cells, cancer-associated macrophages (CAMs; F4/80$^+$ cells) and suppressive myeloid cells also secrete numerous molecules, to directly support activation and survival of stromal cells (Joyce and Pollard, 2009; Beatty *et al.*, 2011; Lu *et al.*, 2011; Coussens *et al.*, 2013; Turley *et al.*, 2015). In the current study, we have discovered that LW106 profoundly inhibits stromal cell recruitment and ECM deposition in the TME, which in turn causes an impaired crosstalk between stromal compartment and T cells, thus promoting T cell immune response to tumours. On the other hand, our data suggest that targeting IDO1 in host-derived cells by LW106 strongly suppresses infiltration of CD4$^+$Foxp3$^+$ regulatory T cells and F4/80$^+$ CAMs (data not shown), which consequently results in an impaired immune-stroma interaction, thus limiting recruitment, activation and survival of stromal cells in the TME. Further work is required to define the precise mechanisms by which LW106 inhibits recruitment, activation and survival of non-haematopoietic stromal cells in the TME. In addition to the immunomodulatory role, stromal compartment in the TME may also have a critical role in controlling CSC expansion (Buckanovich *et al.*, 2008; Joyce and Pollard, 2009). Herein, we demonstrate that the expansion of CSCs is strongly suppressed in tumours of LW106-treated mice, suggesting that the inhibitory effect of LW106 on tumour growth and chemoresistance can, at least in part, be attributed to reduced CSC enrichment in the TME.

In conclusion, the data presented here suggest that LW106 inhibits tumour growth by limiting stroma-immune crosstalk and CSC enrichment in the TME and that LW106 can be further developed as a potential immunotherapeutic agent used in combination with immune checkpoint inhibitors and (or) chemotherapeutic drugs for cancer treatment.

## Acknowledgements

This work was supported by the National Natural Science Foundation of China (81572745, 91539115 and 81603134), the Jiangsu Provincial Natural Science Fund for Distinguished Young Scholar (BK20170029), the Jiangsu Provincial Natural Science Fund for Young Scholar (BK20160758), the Jiangsu Provincial Innovative Research Program, the fund from State Key Laboratory of Natural Medicines of China Pharmaceutical University (SKLNMZZJQ201604) and the fund from Collaborative Innovation Center for Gannan Oil-Tea Camellia Industrial Development (YP201608).

## Author contributions

R.F. designed and performed experiments, analysed data and wrote the paper. Y.-W.Z. and H.-M.L. performed experiments and analysed data. W.-C.L. and L.Z. performed experiments. Q.-L.G., S.J.W. and T.L. provided relevant advice. Z.-Y.L. provided compound. Z.-Q.W. oversaw the project, designed experiments, analysed data and wrote the paper.

## Conflict of interest

The authors declare no conflict of interest.

## Declaration of transparency and scientific rigour

This Declaration acknowledges that this paper adheres to the principles for transparent reporting and scientific rigour of preclinical research recommended by funding agencies, publishers and other organisations engaged with supporting research.

## References

Alexander SPH, Fabbro D, Kelly E, Marrion NV, Peters JA, Faccenda E *et al.* (2017). The Concise Guide to PHARMACOLOGY 2017/18: Enzymes. Br J Pharmacol 174: S272–S359.

Beatty GL, Chiorean EG, Fishman MP, Saboury B, Teitelbaum UR, Sun W *et al.* (2011). CD40 agonists alter tumor stroma and show efficacy against pancreatic carcinoma in mice and humans. Science 331: 1612–1616.

Bhowmich NA, Neilson EG, Moses HL (2004). Stromal fibroblasts in cancer initiation and progression. Nature 432: 332–337.

Botting NP (1995). Chemistry and neurochemistry of kynurenine pathway of tryptophan metabolism. Chem Soc Rev 24: 401–412.

Brandacher G, Perathoner A, Ladurner R, Schneeberger S, Obrist P, Winkler C *et al.* (2006). Prognostic value of indoleamine 2,3-dioxygenase expression in colorectal cancer: effect on tumor-infiltrating T cells. Clin Cancer Res 12: 1144–1151.

Buckanovich RJ, Facciabene A, Kim S, Benencia F, Sasaroli D, Balint K *et al.* (2008). Endothelin B receptor mediates the endothelial barrier to T cell homing to tumors and disables immune therapy. Nat Med 14: 28–36.

Cady SG, Sono M (1991). 1-methyl-DL-tryptophan, β-(3-benzofurany)-DL-alanine, and β-[3-benzo(b)thienyl]-DL-alanine are competitive inhibitors for indoleamine 2,3-dioxygenase. Arch Biochem Biophys 291: 326–333.

Caruana I, Savoldo B, Hoyos V, Weber G, Liu H, Kim ES *et al.* (2015). Heparanase promotes tumor infiltration and antitumor activity of CAR-redirected T lymphocytes. Nat Med 21: 524–529.

Castermans K, Griffioen AW (2007). Tumor blood vessels, a difficult hurdle for infiltrating leukocytes. Biochem Biophys Acta 1776: 160–174.

Codony-Servat J, Verlicchi A, Rosell R (2016). Cancer stem cells in small cell lung cancer. Transl Lung Cancer Res 5: 16–25.

Coussen LM, Werb Z (2002). Inflammation and cancer. Nature 420: 860–867.

Coussens LM, Zitvogel L, Palucka AK (2013). Neutralizing tumor promising chronic inflammation: a magic bullet? Science 339: 286–291.

Curtis MJ, Bond RA, Spina D, Ahluwalia A, Alexander SP, Giembycz MA *et al.* (2015). Experimental design and analysis and their reporting: new guidance for publication in BJP. Br J Pharmacol 172: 3461–3471.

Eleftheriadis T, Pissas G, Antoniadi G, Spanoulis A, Liakopoulos V, Stefanidis L (2014). Indoleamine 2,3-dioxygenase increases p53 levels in alloreactive human T cells, and both indoleamine 2,3-dioxygenase and p53 suppress glucose uptake, glycolysis and proliferation. Int Immunol 26: 673–684.

Fallarino F, Grohmann U, Vacca C, Bianchi R, Orabona C, Spreca A *et al*. (2002). T cell apoptosis by tryptophan catabolism. Cell Death Differ 9: 1069–1077.

Feig C, Jones JO, Kraman M, Wells RJ, Deonarine A, Chan DS *et al*. (2013). Targeting CXCL12 from FAP-expressing carcinoma-associated fibroblasts synergizes with anti-PD-L1 immunotherapy in pancreatic cancer. Proc Natl Acad Sci U S A 110: 20212–20217.

Frumento G, Rotondo R, Tonetti M, Damonte G, Benatti U, Ferrara GB (2002). Tryptophan-derived catabolites are responsible for inhibition of T and natural killer cell proliferation induced by indoleamine 2,3-dioxygenase. J Exp Med 196: 459–468.

Gyorffy B, Lanczky A, Eklund AC, Denkert C, Budczies J, Li Q *et al*. (2010). An online survival analysis tool to rapidly assess the effect of 22,277 genes on breast cancer prognosis using microarray data of 1809 patients. Breast Cancer Res Treat 123: 725–731.

Gyorffy B, Lanczky A, Szallasi Z (2012). Implementing an online tool for genome-wide validation of survival-associated biomarkers in ovarian-cancer using microarray data of 1287 patients. Endocr-Relat Cancer 19: 197–208.

Gyorffy B, Surowiak P, Budczies J, Lanczky A (2013). Online survival analysis software to assess the prognostic value of biomarkers using transcriptomic data in non-small-cell lung cancer. PLoS ONE 8: e82241.

Hanahan D, Coussens LM (2012). Accessories to the crime: functions of cells recruited to the tumor microenvironment. Cancer Cell 21: 309–322.

Hardavella G, George R, Sethi T (2016). Lung cancer stem cells-characteristics, phenotype. Transl Lung Cancer Res 5: 272–279.

Harding SD, Sharman JL, Faccenda E, Southan C, Pawson AJ, Ireland S *et al*. (2018). The IUPHAR/BPS guide to PHARMACOLOGY in 2018: updates and expansion to encompass the new guide to IMMUNOPHARMACOLOGY. Nucl Acids Res 46: D1091–D1106.

Hanahan D, Weinberg RA (2011). Hallmarks of cancer: the next generation. Cell 144: 646–674.

Holmgaard RB, Zamarin D, Munn DH, Wolchok JD, Allison JP (2013). Indoleamine 2,3-dioxygenase is a critical resistance mechanism in antitumor T cell immunotherapy targeting CTLA-4. J Exp Med 210: 1389–1402.

Ino K, Yamamoto E, Shibata K, Kajiyama H, Yoshida N, Terauchi M *et al*. (2008). Inverse correlation between tumoral indoleamine 2,3-dioxygenase expression and tumor-infiltrating lymphocytes in endometrial cancer: its association with disease progression and survival. Clin Cancer Res 14: 2310–2317.

Jackson E, Dees EC, Kauh JS, Harvey RD, Neuger A, Lush R *et al*. (2013). A phase I study of indoximod in combination with docetaxel in metastatic solid tumors. 2013 ASCO Annual Meeting. J Clin Oncol 31 (suppl) abstr 3026.

Johansson M, Denardo DG, Coussens LM (2008). Polarized immune responses differentially regulate cancer development. Immunol Rev 222: 145–154.

Joyce JA, Pollard JW (2009). Microenvironmental regulation of metastasis. Nat Rev Cancer 9: 239–252.

Kilkenny C, Browne W, Cuthill IC, Emerson M, Altman DG (2010). Animal research: reporting *in vivo* experiments: the ARRIVE guidelines. Br J Pharmacol 160: 1577–1579.

Liu X, Shin N, Koblish HK, Yang G, Wang Q, Wang K *et al*. (2010). Selective inhibition of IDO1 effectively regulates mediators of antitumor immunity. Blood 115: 3520–3530.

Lu P, Takai K, Weaver VM, Werb Z (2011). Extracellular matrix degradation and remodeling in development and disease. Cold Spring Harb Perspect Biol 3: a005058.

Mellor AL, Baban B, Chandler P, Marshall B, Jhaver K, Hansen A *et al*. (2003). Induced indoleamine 2,3 dioxygenase expression in dendritic cell subsets suppresses T cell clonal expansion. J Immunol 171: 1652–1655.

McGrath JC, Lilley E (2015). Implementing guidelines on reporting research using animals (ARRIVE etc.): new requirements for publication in BJP. Br J Pharmacol 172: 3189–3193.

Munn DH, Mellor AL (2004). IDO and tolerance to tumors. Trans. Mol Med 10: 15–18.

Munn DH, Mellor AL (2007). Indoleamine 2,3-dioxygenase and tumor-induced tolerance. J Clin Invest 117: 1147–1154.

Munn DH, Shafizadeh E, Attwood JT, Bondarev I, Pashine A, Mellor AL (1999). Inhibition of T cell proliferation by macrophage tryptophan catabolism. J Exp Med 189: 1363–1372.

Munn DH, Sharma MD, Baban B, Harding HP, Zhang Y, Ron D *et al*. (2005). GCN2 kinase in T cells mediates proliferative arrest and anergy induction in response to indoleamine 2,3-dioxygenase. Immunity 22: 633–642.

Munn DH, Sharma MD, Lee JR, Jhaver KG, Johnson TS, Keskin DB *et al*. (2002). Potential regulatory function of human dendritic cells expressing indoleamine 2,3-dioxygenase. Science 297: 1867–1870.

Ni T, Li X-Y, Lu N, An T, Liu Z-P, Fu R *et al*. (2016). Snail1-dependent p53 repression regulates expansion and activity of Tumor-initiating cells in breast cancer. Nat Cell Biol 18: 1221–1232.

Pan K, Wang H, Chen MS, Zhang HK, Weng DS, Zhou J *et al*. (2008). Expression and prognosis role of indoleamine 2,3-dioxygenase in hepatocellular carcinoma. J Cancer Res Clin Oncol 134: 1247–1253.

Polak ME, Borthwich NJ, Gabriel FG, Johnson P, Higgins B, Hurren J *et al*. (2007). Mechanisms of local immunosuppression in cutaneous melanoma. Br J Cancer 96: 1879–1887.

Prendergast GC (2008). Immune escape as a fundamental trait of cancer: focus on IDO. Oncogene 27: 3889–3900.

Provenzano PP, Cuevas C, Chang AE, Goel VK, Von Hoff DD, Hingorani SR (2012). Enzymatic targeting of the stroma ablates physical barriers to treatment of pancreatic ductal adenocarcinoma. Cancer Cell 21: 418–429.

Salmon H, Franciszkiewicz K, Damotte D, Dieu-Nosjean MC, Validire P, Trautmann A *et al*. (2012). Matrix architecture defines the preferential localization and migration of T cells into the stroma of human lung Tumors. J Clin Invest 122: 899–910.

Sono M, Hayaishi O (1980). The reaction mechanism of indoleamine 2,3-dioxygenase. Biochem Rev 50: 173–181.

Sono M, Roach MP, Coulter ED, Dawson JH (1996). Heme-containing oxygenases. Chem Rev 96: 2841–2888.

Szasz AM, Lanczky A, Nagy A, Forster S, Hark K, Green JE *et al*. (2016). Cross-validation of survival associated biomarkers in gastric cancer using transcriptomic data of 1,065 patients. Oncotarget 7: 49322–49333.

Tan W, Zhang W, Strasner A, Grivennikov S, Cheng JQ, Hoffman RM *et al*. (2011). Tumor-infiltrating regulatory T cells stimulate mammary cancer metastasis through RANKL-RANK signaling. Nature 470: 548–553.

Turley SJ, Cremasco V, Astarita JL (2015). Immunological hallmarks of stromal cells in the tumor microenvironment. Nat Rev Immunol 15: 669–682.

## Supporting Information

Additional supporting information may be found online in the Supporting Information section at the end of the article.

https://doi.org/10.1111/bph.14351

**Figure S1** Chemical structure of LW106. Dashed area represents structural modification of lead compound 62.

**Figure S2** Tumor cell-derived *IDO1* expression level does not correlate with survival of two subtypes of lung cancer patients. Kaplan–Meier survival analysis of the relationship between survival rates and tumor cell-derived *IDO1* expression level in two subtypes of lung cancer patients. (A, B) Relationship between overall survival (OS) rate and *IDO1* expression level in lung adenocarcinoma (A) and squamous (B) patients. (C, D) Relationship between post-progression survival (PPS) rate and *IDO1* expression level in lung adenocarcinoma (C) and squamous (D) patients. Differences between two survival curves are measured by Log-Rank Test. *n* represents the number of patients.

**Figure S3** LW106 treatment inhibits IDO1 enzyme activity but does not affect tumor cell proliferation *in vitro*. (A) Inhibition rate of kynurenine (Kyn) for IFN-γ- stimulated HeLa cells that were treated with indicated concentrations of LW106 for 48 hrs ($n$ = 3 independent experiments). (B) Western blot analysis of IDO1 protein levels for IFN-γ-stimulated HeLa cells that were treated with indicated compounds (results are representatives of three experiments). (C) Survival rate of indicated tumor cells that were treated with increasing doses of LW106. Cells were stained with trypan blue dye and the staining exclusive cells (*i.e*. live cells) were counted under light microscope. $n$ = 3 independent experiments. (D) Representative images of cells as described in C. (E) Western blot analysis of IDO1 protein levels for B16F10 and Lewis cells (results are representatives of three experiments).

**Figure S4** LW106 treatment reverses CD8+ T-cell suppression mediated by IDO1+ mature DCs. IDO1- immature DCs were treated with 50 ng/ml hIFN-γ and 1 μg/ml LPS for 2 days, and the obtained IDO1+ mature DCs or IDO1- immature DCs were cocultured with purified lymphocytes in the presence of vehicle, LW106 or epacadostat for additional 2 days. Co-cultured cells were harvested, stained with anti-CD8 antibody and subjected to FACS analysis. (A) Representative plot of FACS analysis. (B) Percentage of CD8+ T cells in the co-culture system as described in A. n = 3 independent experiments. Statistical significance was evaluated by two-way ANOVA test (*$P < 0.05$; **$P < 0.01$).

**Figure S5** LW106 treatment does not induce histological change in tumorbearing mice. (A, B) H.E. staining of vital organs from LW106-trated mice bearing with Lewis tumor cells (A) and B16F10 melanoma cells (B). Images are representative of images from six mice.

**Figure S6** LW106 treatment enhances infiltration and accumulation of T cells in B16F10 tumors. B16F10 xenografts from vehicle-, LW106- and epacadostat-treated mice were harvested 18 days after tumor challenge and subjected to FACS and immunofluorescent analyses. (A) Representative dot plots and percentage of CD8+ effector T cells of total CD45+ cells for vehicle-, LW106- and epacadostat-treated mice ($n$ = 5 mice, each). (B) Percentage of CD4 + Foxp3+ regulatory T cells expressing Ki67 for indicated mice as shown in *A*. (C) Ratio of CD4 + Foxp3- effector T cells to CD4 + Foxp3+ regulatory T cells in tumors of indicated mice as shown in *A*. (D) Representative immunofluorescent images (*left panels*; images are representative of images from five mice) and percentage of CD8+ T cells expressing Ki67 for tumors of indicated mice (*right panel*; 1000 ~ 2000 cells were counted in 10 random fields of each slide). Arrow head denotes Ki67 + CD8+ cells. Statistical significance was evaluated by two-way ANOVA test (*$P < 0.05$; **$P < 0.01$; #$P < 0.05$; N.S., not significant).

**Figure S7** LW106 treatment results in impaired proliferation and survival of B16F10 melanoma cells in tandem with reduced recruitment of tumor-associated stromal cells and deposition of extracellular matrix. B16F10 xenografted tumors from vehicle-, LW106- and epacadostat-treated mice were harvested 18 days after tumor challenge and analyzed by immunohistochemistry. (A) Representative immunohistochemical images (*left panels*; images are representative of images from six mice) and percentages of Ki67-, phospho-histone H3- and cleaved caspase 3-positive cells for tumors of indicated mice (*right panels*; 1000 ~ 2000 cells were counted in 10 random fields of each slide). (B) Representative immunofluorescent images (*left panels*; images are representative of images from six mice) and relative fluorescent intensities of type I collagen, CD31 and α-SMA (*right panels*; relative fluorescent intensities were calculated in 10 random fields of each slide) for tumors of indicated mice ($n$ = 6 mice, each). Statistical significance was evaluated by two-way ANOVA test (*$P < 0.05$; **$P < 0.01$; ***$P < 0.001$; N.S., not significant).